

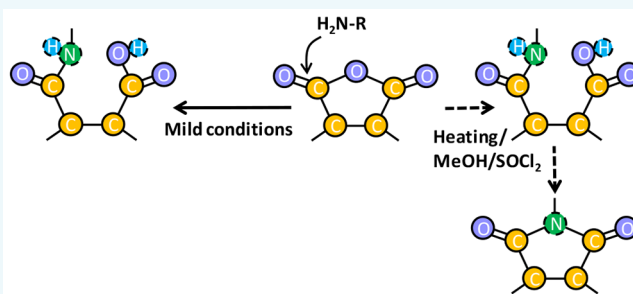
# Modification of Poly(maleic anhydride)-Based Polymers with H<sub>2</sub>N–R Nucleophiles: Addition or Substitution Reaction?

Zhicheng Jin, Liang Du, Chengqi Zhang, Yuya Sugiyama,<sup>†</sup> Wentao Wang,<sup>‡</sup> Goutam Palui,<sup>§</sup> Sisi Wang, and Hedi Mattoussi<sup>\*†</sup>

Department of Chemistry and Biochemistry, Florida State University, 95 Chieftan Way, Tallahassee, Florida 32306, United States

## S Supporting Information

**ABSTRACT:** Reacting poly(maleic anhydride)-based polymers with H<sub>2</sub>N–R nucleophiles is a flexible and highly effective approach for preparing a variety of multifunctional, multicoordinating, and multireactive polymers. The exact transformation of the anhydride ring during this addition reaction is still an open question. In this report, we characterize the transformation of a representative block copolymer, poly(isobutylene-*alt*-maleic anhydride), with a few H<sub>2</sub>N–R nucleophiles. In particular, we test the effects of varying a few reaction parameters/conditions (e.g., temperature, solvent, reaction time, and addition of thionyl chloride) on the nature of the anhydride transformation and bond formed between the polymer and the lateral R groups. The resulting polymers are characterized using a combination of analytical techniques including FT-IR, one- and two-dimensional NMR, and gel electrophoresis. We find that the ring opening transformation occurs under mild conditions. Conversely, cyclic imide transformation can take place for reactions carried out at high temperature (e.g., in DMF under refluxing conditions). We also find that use of a protic solvent, such as methanol, or addition of thionyl chloride (SOCl<sub>2</sub>) to the reaction mixture under refluxing conditions can promote cyclic imide transformation. The cyclic imide transformation is nonetheless partial, as carboxyl groups could still be accounted for in the resulting compounds. Depending on the type of transformation, the resulting polymer can exhibit a few distinct properties, such as net charge buildup along the chain, or the appearance of weak UV–vis absorption and fluorescence properties. These findings are useful for understanding the properties exhibited by polymer materials prepared via this flexible and highly effective route using anhydride containing polymers and oligomers.



## INTRODUCTION

Poly(maleic anhydride)-based polymers, often used as block copolymers, have provided chemists with a great platform for introducing a variety of lateral functionalities along a polymer backbone, yielding multifunctional materials that have found use in a wide range of applications.<sup>1–6</sup> This is facilitated by the effectiveness of reacting anhydride rings with nucleophilic molecules (e.g., H<sub>2</sub>N–R), via the reagent-free nucleophilic attack. As such, the transformation of various poly(maleic anhydride)-based compounds with an array of amine-terminated groups has allowed the preparation of multifunctional polymers that have found use in the surface coating and functionalization of colloidal nanomaterials,<sup>1,4,6–10</sup> the design of drug delivery vehicles,<sup>2,11</sup> and the preparation of antibacterial agents.<sup>3</sup> For instance, the groups of Parak and co-workers and Colvin and co-workers have exploited this reaction route to transform poly(maleic anhydride-*alt*-1-octadecene), PMAO, into amphiphilic polymers suited for encapsulating colloidal semiconductor nanocrystals (quantum dots, QDs) and iron oxide nanoparticles (IONPs).<sup>12,13</sup> Starting with poly(isobutylene-*alt*-maleic anhydride), PIMA, we have used the nucleophilic addition reaction to prepare a set of hydrophilic multicoordinating ligands and applied them to coat

various colloidal nanocrystals (e.g., Au nanostructures, luminescent QDs, and IONPs).<sup>6,10,14</sup> Conversely, Halder and co-workers exploited this transformation reaction, applied to PIMA, to prepare a set of cationic polymers as mimics of antimicrobial peptides and tested their effectiveness against pathogenic bacteria.<sup>3</sup>

Many of the reported studies have described the reaction of anhydride rings with functional amines as a ring opening transformation, producing amide linked pendant groups combined with the release of carboxylic acid groups along a polymer chain.<sup>1,4,10</sup> Nonetheless, a few literature studies have actually discussed the transformation reaction as substitution (imidization) where the lateral groups are directly bound to the anhydride rings, and without the release of carboxylic acids (see Figure 1).<sup>3,15–17</sup> Such interpretation has been challenged in subsequent work, nonetheless.<sup>18</sup> Additionally, the characterization of the polymer products was based on limited analytical measurements, most of them using FT-IR spectroscopy.

Received: January 5, 2019

Revised: February 9, 2019

Published: February 14, 2019

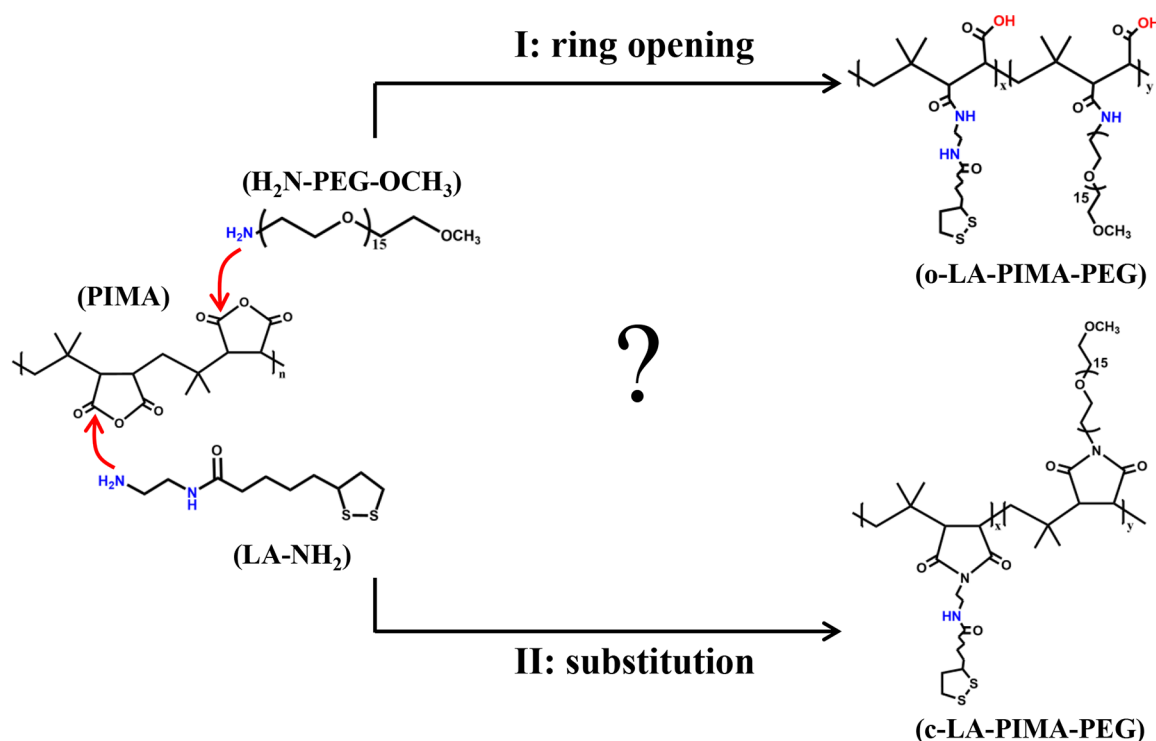


**Figure 1.** Schematic representation showing the addition reaction between poly(isobutylene-*alt*-maleic anhydride) and H<sub>2</sub>N-R motifs (R = PEG-OMe or/and LA). The two proposed pathways describing (I) anhydride ring opening coupled with amide-bond formation with R, or (II) substitution reaction yielding cyclic imide-bound R.

In this study, we test the effects of varying several conditions, for the addition reaction applied to PIMA (serving as a precursor), on the nature of the anhydride transformation and the resulting bond between the backbone and the installed H<sub>2</sub>N-R groups. We apply several characterization techniques to identify the correlation between the reaction conditions used (e.g., temperature, reaction time, and solvent) and the nature of the bond holding the pendant groups. We find that most of the reaction conditions, routinely used by various groups, yield open ring structure, with an amide bond coupling the R groups to the polymer, along with the freeing of several carboxylic acid groups. In contrast, the closed ring structure can occur under limited conditions, namely for reactions carried out under high temperature and/or with the introduction of thionyl chloride (SOCl<sub>2</sub>). Our data have also provided additional insights into the steps involved in the imidization reaction. They show that the transformation may actually involve a ring opening (as a first step) followed by progressive ring closing after extended reaction time. Ring closing reaction is not fully complete, however, as a small fraction of open ring structures can still be measured.

## RESULTS AND DISCUSSION

**Rationale.** The main motivation of this report is to provide a clear picture of the transformation of the anhydride (succinic anhydride) rings along a polymer chain during the reaction with any H<sub>2</sub>N-R nucleophiles (see schematic representation in Figure 1). Though the reaction ultimately leads to the coupling of the lateral R groups onto the backbone, the property of the resulting compound can be strongly affected by the exact nature of the transformation. For instance, a ring opening reaction produces several carboxylic acids (one per anhydride ring), while providing R groups coupled to the chain

via amide bonds. The freed carboxyl groups provide an overall charge, which could affect the hydrophilicity and reactivity of the final compound. In contrast, a reaction involving substitution yields R groups bound to the backbone via a cyclic imide and without the generation of carboxylic acid groups. Clearly, there are chemical ramifications of the exact transformation on the properties of the final compound.

To address this question, we carried out the transformation reaction of poly(isobutylene-*alt*-maleic anhydride) with amine-terminated poly(ethylene glycol) or/and lipoic acid (H<sub>2</sub>N-R, R = PEG<sub>750</sub>-OCH<sub>3</sub> or/and LA) by varying a few critical parameters, namely, temperature of the reaction, solvent, reaction time, and the presence of SOCl<sub>2</sub>, and probed the exact structure of the final polymer using mainly FT-IR spectroscopy. The FT-IR results were further supported by 1-D <sup>1</sup>H and 2-D cross-correlation NMR spectroscopy measurements. Additionally, we used gel electrophoresis experiments to verify the presence of carboxyl groups along the modified macromolecules. We present the data collected from the transformation of PIMA (as a model system) but our findings can be extended to other polymers presenting the anhydride motifs in their macromolecular structures.

**Effects of Varying the Reaction Temperature.** The effects of temperature have been tested by carrying out the reaction in DMF either at a temperature range of ~40–70 °C (i.e., mild heating) or at 153 °C (i.e., refluxing conditions). We focus on these “extreme” conditions, because they were reported to yield two structurally distinct polymers.<sup>1,6,13,17,19</sup> We will refer to the resulting compounds with open ring structures as o-X (e.g., o-PIMA-PEG or o-LA-PIMA-PEG). Conversely, compounds referred to as c-X (e.g., c-PIMA-PEG or c-LA-PIMA-PEG) indicate structures with anticipated closed cyclic imide rings along the chain. The chemical

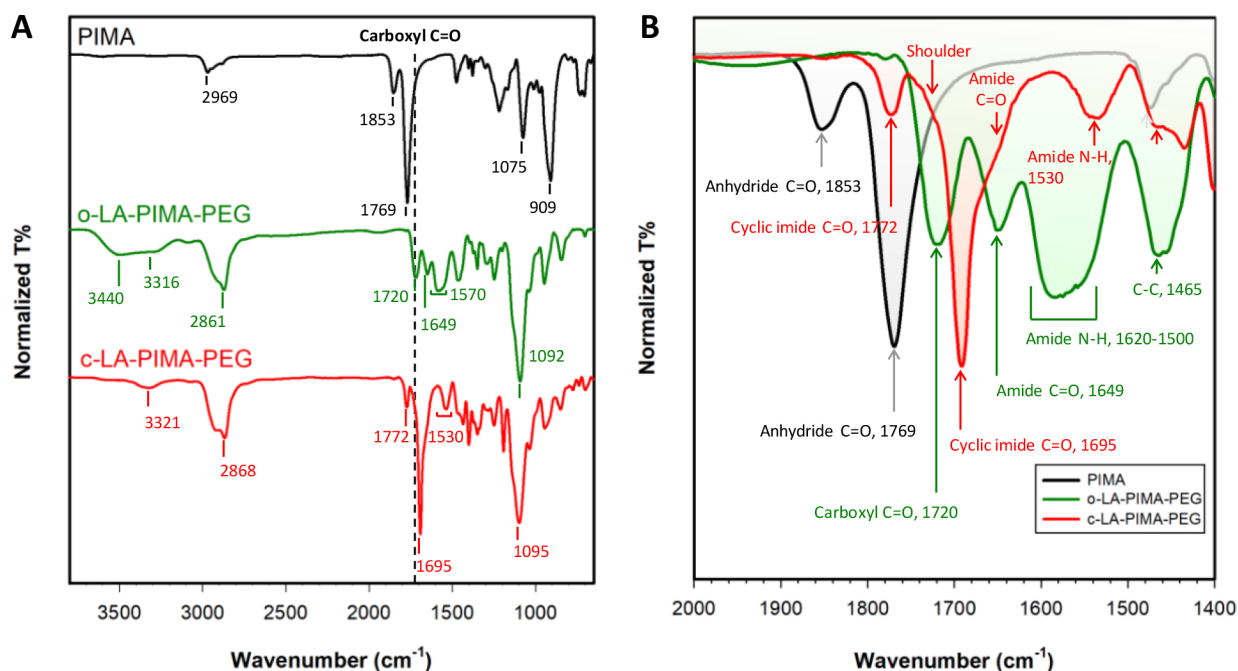


**Figure 2.** Panel A shows the FT-IR spectra over the range 3800–650  $\text{cm}^{-1}$  collected from the native PIMA (black curve); o-LA-PIMA-PEG, prepared using mild reaction conditions (low temperature, green curve); and c-LA-PIMA-PEG, prepared at high temperature (refluxing in DMF, red curve). The dashed line indicates the signature of carbonyl ( $\text{C}=\text{O}$  at 1720  $\text{cm}^{-1}$ ) group in the carboxylic acid. Panel B shows a close-up of those spectra over range 2000–1400  $\text{cm}^{-1}$ , where the  $\text{C}=\text{O}$  signatures are associated with the anhydride ring (black curve), the carboxyl or/and the amide groups (green curve), and the cyclic imide (red curve).

structures of the final products are identified by FT-IR and NMR spectroscopy.

Figure 2 panel A shows a side-by-side comparison between the FT-IR spectra collected from the various compounds over a broad range (3800–650  $\text{cm}^{-1}$ ) that includes vibrations associated with the O–H, C=O, and C–O–C stretching modes (see Table 1). Conversely, panel B shows the same FT-IR spectra but over a narrow window (2000–1400  $\text{cm}^{-1}$ ), mainly focusing on the vibrations associated with the carbonyl ( $\text{C}=\text{O}$ ) group. A close inspection of the data from the PIMA precursor and from the compounds generated using reactions carried out at low temperature (compare black and green profiles, respectively) strongly suggest that a ring opening transformation has taken place. This conclusion is based on the following three observations: (1) Formation of  $-\text{COOH}$  is reflected by the shift of the  $\text{C}=\text{O}$  wavenumbers from 1853 and 1769  $\text{cm}^{-1}$  (ascribed to the symmetric and asymmetric stretching modes in the anhydride rings of the PIMA) to 1720  $\text{cm}^{-1}$  (ascribed to the  $\text{C}=\text{O}$  stretching in the protonated carboxylic acid). Along with those signatures, a broad band at 3500–3100  $\text{cm}^{-1}$  ascribed to O–H stretching is also measured. (2) Formation of the amide bond ( $-\text{CONH}-$ ) is accounted for by the emergence of two bands at 1649  $\text{cm}^{-1}$  and 1620–1500  $\text{cm}^{-1}$ , respectively, assigned to the  $\text{C}=\text{O}$  stretching and N–H bending vibrations. (3) There are no measurable signals that can be ascribed to cyclic anhydride (at 1769 or 1853  $\text{cm}^{-1}$ ) or cyclic imide (at 1695  $\text{cm}^{-1}$ , see below) in the product, which proves that no ring closing has taken place for reactions carried out under mild conditions (i.e., slight heating). Details about the assignments of symmetric and asymmetric  $\text{C}=\text{O}$  stretching in the cyclic anhydride or the imide are provided in the Supporting Information (Figure S1).

**Table 1. Characteristic FT-IR Bands**

Wavenumber range, $\text{cm}^{-1}$	Function class	Assignment	References
3500–2500	carboxylic acid	O–H stretching, broad feature; 2° N–H stretching	22, p. 313; 340
3000–2850	alkane	C–H stretching, 2 bands	22, p. 218
1857–1853; 1769	cyclic anhydride	symmetric C=O stretching; asymmetric C=O stretching	20, p. 130; 22, p. 311
1730–1724	ester	C=O stretching	20, p. 132; 22, pp. 301–305
1720–1707	carboxylic acid	C=O stretching	20, p. 125
1768; 1695	cyclic imide	symmetric C=O stretching; asymmetric C=O stretching	22, p. 324
1649; 1620–1500	amide	C=O stretching; 2° N–H bending	22, p. 319
1575	sodium carboxylate	C=O stretching	22, p. 318
1191	cyclic imide	C–3° N(CH <sub>2</sub> )–C stretching	20, p. 110; 22, p. 341
1100–1092	ethylene glycol	C–O–C stretching	20, p. 102; 22, p. 336
1075–1071; 922–909	cyclic anhydride	C–O–C stretching	22, p. 312

In comparison, the FT-IR spectra collected from the compounds generated using a reaction at 153 °C (red curve) show two well-defined peaks at 1772 and 1695  $\text{cm}^{-1}$ , ascribed to the symmetric and asymmetric  $\text{C}=\text{O}$  stretching modes in the cyclic imide (anticipated for the c-X compounds). However, for reaction carried at high temperature, the cyclic

Table 2. Synthesis of LA-PIMA-PEG Ligand under Different Reaction Conditions

Entry	Solvent	Temperature	Time	SOCl <sub>2</sub>	Ring-closing	Analytical technique used
1	DMF <sup>a</sup>	65 °C	24 h	No	No	FT-IR, NMR, UV–vis, PL
2	DMF <sup>b</sup>	65 °C	96 h	No	No	FT-IR
3	DMF <sup>a</sup>	153 °C, reflux	24 h	No	Nearly all	FT-IR, NMR, UV–vis, PL
4	DMF <sup>b</sup>	153 °C, reflux	96 h	No	Partial	FT-IR
5	Methanol <sup>b</sup>	64 °C, reflux	96 h	No	Partial	FT-IR
6	Methanol <sup>b</sup>	64 °C, reflux	2 h	1.5 equiv	Partial	FT-IR
7	CHCl <sub>3</sub> <sup>b</sup>	61 °C, reflux	96 h	No	No	FT-IR
8	CHCl <sub>3</sub> <sup>b</sup>	61 °C, reflux	24 h	1.5 equiv	Partial	FT-IR
9	CH <sub>2</sub> Cl <sub>2</sub> <sup>b</sup>	40 °C, reflux	24 h	No	No	FT-IR
10	CH <sub>2</sub> Cl <sub>2</sub> <sup>b</sup>	40 °C, reflux	96 h	No	No	FT-IR

<sup>a</sup>Synthesis from precursors (i.e., PIMA, LA-NH<sub>2</sub>, and H<sub>2</sub>N-PEG-OMe). <sup>b</sup>Reaction from presynthesized o-LA-PIMA-PEG ligand.

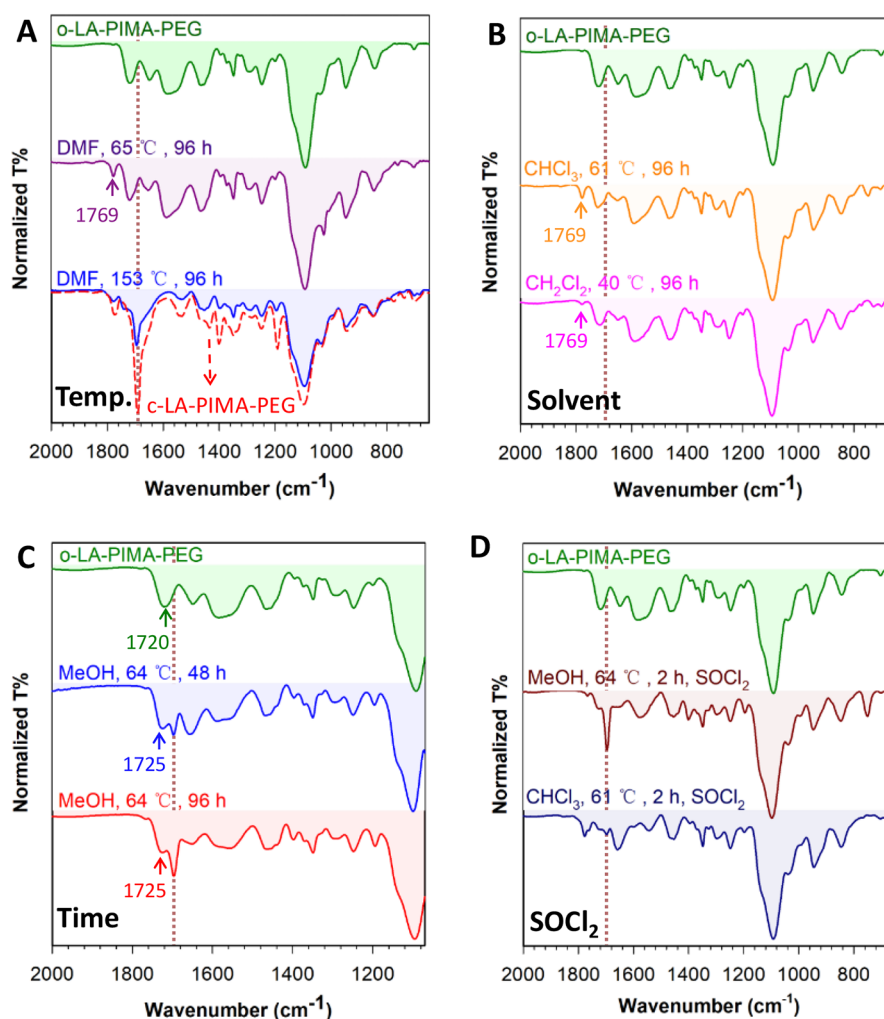


**Figure 3.** FT-IR spectra collected from pre-synthesized o-LA-PIMA-PEG polymer subjected to various treatments, as detailed in each panel: heating at different temperatures, refluxing in different chlorinated solvents, refluxing for different times in methanol, and refluxing in different solvents and in the presence of added SOCl<sub>2</sub>. Note that the dashed red spectrum in panel A, collected from the compound c-LA-PIMA-PEG, is reproduced from Figure 2. The dashed lines in all the panels designate the location of the asymmetric C=O stretching mode (at 1695 cm<sup>-1</sup>) expected in the cyclic imides.

imide transformation is not 100% complete, since the FT-IR spectrum shows a shoulder at 1720 cm<sup>-1</sup> (next to the C=O peak at 1695 cm<sup>-1</sup>) ascribed to carboxyl groups. This finding is consistent with additional FT-IR data collected from a pure c-PIMA-PEG (melt), prepared by carrying the reaction under vacuum at 150 °C for 24 h.<sup>23</sup> The spectrum shows a weak signal ascribed to the amide N–H bending at 1600 cm<sup>-1</sup>,

which implies that open ring structures persist for reactions carried out in melt conditions. More details are available in the Supporting Information (Figure S1B, light brown profile). We should note that the signatures measured from the amide C=O (at 1649 cm<sup>-1</sup>) and N–H (at 1530 cm<sup>-1</sup>) in the c-LA-PIMA-PEG shown in Figure 2, but are much weaker in the melt c-PIMA-PEG, are ascribed to the amide bond in the LA-





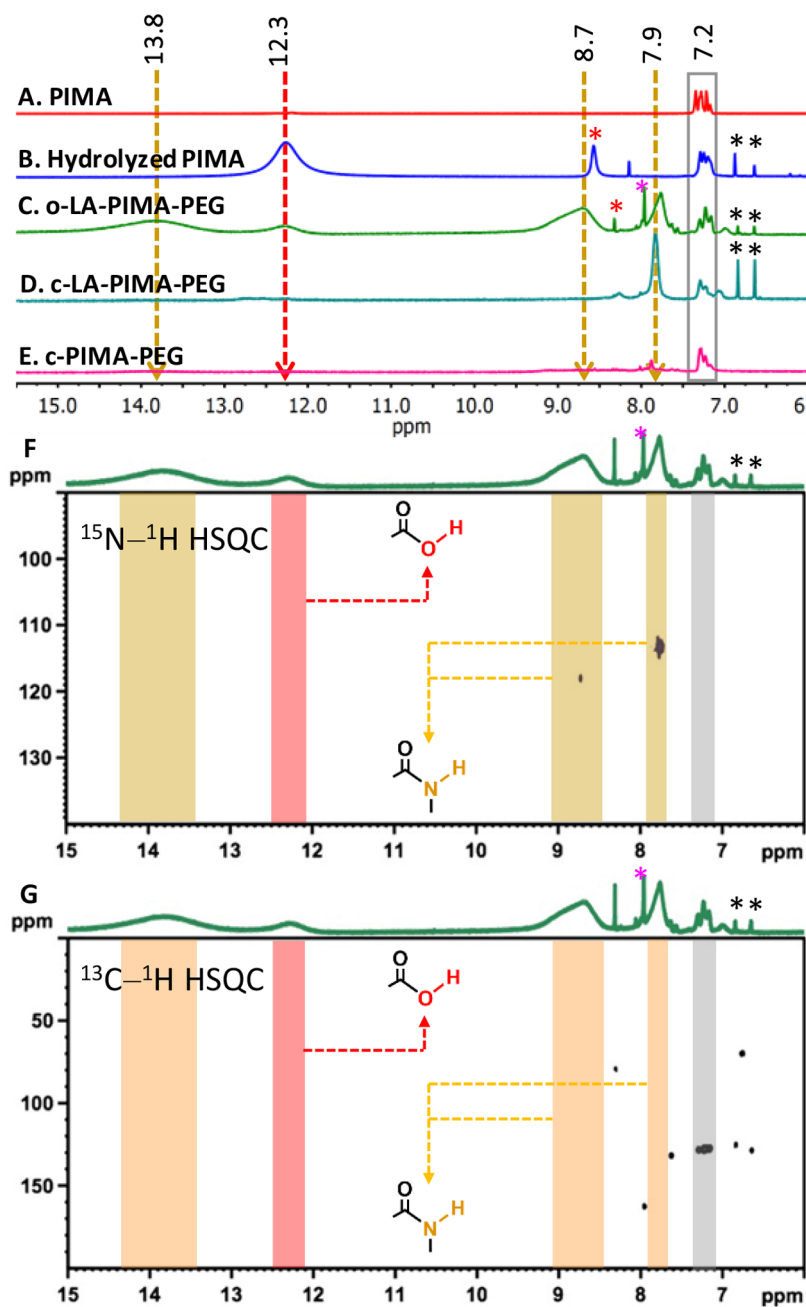


**Figure 5.**  $^1\text{H}$  NMR spectra of (A) PIMA precursor; (B) hydrolyzed PIMA; (C) o-LA-PIMA-PEG; (D) c-LA-PIMA-PEG; and (E) c-PIMA-PEG. (F) 2-D  $^{13}\text{C}$ - $^1\text{H}$  HSQC spectrum collected from o-LA-PIMA-PEG. (G) 2-D  $^{15}\text{N}$ - $^1\text{H}$  HSQC spectrum of o-LA-PIMA-PEG. Spectra were collected in  $\text{DMSO}-d_6$  solutions. The sharp peak at 8.0 ppm (\*) measured in spectrum C is ascribed to DMF. The peaks at 6.6 and 6.8 ppm (\*) in profiles B, C, and D are from trace amounts of impurities containing conjugated structures (i.e., butylated hydroxytoluene, BHT). The  $^1\text{H}$  signatures (\*) at 8.6 ppm in profile B and at 8.3 ppm in profile C cannot be assigned.

temperatures of  $\text{CHCl}_3$  or  $\text{CH}_2\text{Cl}_2$  are not high enough to promote the intramolecular condensation of o-LA-PIMA-PEG. Note the presence of a small peak at  $1769\text{ cm}^{-1}$  measured in both solvents is attributed to the presence of a few reconstituted anhydride rings, as discussed above.

However, heating the starting compound (o-LA-PIMA-PEG) in methanol yielded slightly different materials. Figure 3 panel C shows that refluxing the solution (at  $64\text{ }^\circ\text{C}$ ) for 48 h resulted in the appearance of a  $\text{C}=\text{O}$  band at  $1695\text{ cm}^{-1}$  in the FT-IR spectrum (anticipated for c-LA-PIMA-PEG). Furthermore, the peak intensity increased for longer refluxing time (96

h, red profile). The spectra also show that the carboxyl  $\text{C}=\text{O}$  stretching band shifted from  $1720$  to  $1725\text{ cm}^{-1}$ , which can be attributed to the formation of ester carbonyl groups between carboxylic acids and solvent molecules. These changes indicate that a slow, though partial, transformation via an esterification step to cyclic imides along the chain takes place when o-LA-PIMA-PEG is heated in methanol (see below discussion and schematics in Figure 4). Nonetheless, a full substitution is not achieved even after refluxing for 96 h, in agreement with the data collected in DMF (see panel A).

The effects of heating the starting compound in methanol can further be enhanced in the presence of  $\text{SOCl}_2$ . Indeed, thionyl chloride has been reported to react with certain solvent molecules. For instance, it reacts with alcohols ( $\text{RCH}_2\text{OH}$ ,  $\text{R} = \text{H}$ ,  $\text{CH}_3$ , or alkyl chain) to yield alkyl chlorides ( $\text{RCH}_2\text{Cl}$ ), or with carboxylic acids ( $\text{R-COOH}$ ) to produce acyl (or acid) chlorides ( $\text{R-COCl}$ ).<sup>25</sup> To test this, 1.5 equiv of  $\text{SOCl}_2$  with respect to the molar concentration of  $-\text{COOH}$  (in o-LA-PIMA-PEG) was added to the methanol or chloroform solution, and the reaction was further refluxed for 2 h. Figure 3 panel D shows that the final product obtained from heating the reaction mixture in methanol solution has an intense and well-defined signature at  $1695\text{ cm}^{-1}$ , ascribed to the asymmetric  $\text{C}=\text{O}$  mode in the cyclic imide, combined with weakening of the  $\text{C}=\text{O}$  signature at  $\sim 1720\text{ cm}^{-1}$  (brown spectrum). Conversely, addition of  $\text{SOCl}_2$  to a solution of o-LA-PIMA-PEG in  $\text{CHCl}_3$  yielded a weak signal at  $1695\text{ cm}^{-1}$  (in the dark blue spectrum), indicating the formation of a rather small fraction of cyclic imides; this feature was not measured in the absence of thionyl chloride (see panel B).

The formation of cyclic imides in methanol solution (requiring more than 48 h, see panel C) can be attributed to esterification of the carboxyl by methanol, which is facilitated by the presence of several carboxyl protons along the polymer chain. This esterification allows the amide (a weak nucleophile) to react with the proximal ester group, ultimately leading to the formation of closed ring structure (see schematics in Figure 4). Conversely, adding  $\text{SOCl}_2$  to a solution of o-LA-PIMA-PEG in methanol rapidly forms methyl chloride, an intermediate substrate that can promote esterification of the carboxyl along the chain (to form  $-\text{COOCH}_3$ ). This in turn accelerates the imidization reaction (as depicted in Figure 4). The addition of  $\text{SOCl}_2$  to o-LA-PIMA-PEG in  $\text{CHCl}_3$ , in comparison, promotes the formation of acid chloride along the polymer backbone,<sup>26</sup> which favors imidization reaction since  $-\text{Cl}$  is a better leaving group than  $-\text{OH}$  (Figure 4). Nonetheless, the rather inefficient ring closing observed for the reaction in  $\text{CHCl}_3$  is caused by absence of any catalytic amount of base.<sup>26</sup> Further details on the reaction of methanol with thionyl chloride to produce methyl chloride and the formation of acid chloride in  $\text{CHCl}_3$  are provided in the Supporting Information (Figure S2).

**NMR Characterization of the Polymer Compounds.** The FT-IR data have been complemented with additional characterization using  $^1\text{H}$  NMR spectroscopy. In particular, we were interested in verifying whether the presence of amide and carboxy (labile) protons in the compounds with open ring structure (e.g., o-LA-PIMA-PEG) is unequivocal or not. Simultaneously, we wanted to show that those protons are conspicuously absent from the compounds with close ring structure. For this,  $^1\text{H}$  NMR spectra were collected from solutions of all the compounds in  $\text{DMSO}-d_6$ . In addition, 2-D heteronuclear single quantum coherence (HSQC,  $^1\text{H}-^{13}\text{C}$  and  $^1\text{H}-^{15}\text{N}$ ) measurements were limited to o-LA-PIMA-PEG ligand, as this compound is expected to contain labile protons, while the closed ring structure compound is not. We note that the protons associated with carboxylic acid ( $-\text{OH}$ ) or amide bond ( $-\text{NH}-$ ) produce chemical shifts  $\delta > 6\text{ ppm}$ , while the carbon-attached protons (methyl, methylene, and methine in the PIMA, LA, and PEG) have chemical shifts  $\delta < 6\text{ ppm}$ ; a full range spectrum collected from o-LA-PIMA-PEG is shown in Figure S3. Details on the peak assignments ( $\delta < 6\text{ ppm}$ ) and integration values are provided in the Supporting Information.

The spectra shown in Figure 5A–E indicate that the multippeak signature at 7.2 ppm measured for the PIMA precursor is also present in the spectra collected from each compound prepared and tested. This signature is not attributed to any of the expected protons in the polymer. It can be ascribed to the terminal benzene ring protons generated from benzoyl peroxide initiator used in the synthesis of PIMA, and will serve as a reference.<sup>27</sup> A few salient features in the spectra shown in Figure 5A–E can be noted. (a) The peak at 12.3 ppm is ascribed to the  $-\text{COOH}$  protons; this signature is more pronounced in the hydrolyzed PIMA than in o-LA-PIMA-PEG, given the larger number of carboxyl groups per polymer generated following hydrolysis (compare profiles Figure 5B and C).<sup>2,28</sup> (b) There are two types of amide protons present in the modified polymer compounds. One is present in the LA- $\text{NH}_2$  precursor and the other is formed during the addition reaction between the anhydride rings and amine-R (see Figure 1). The proton signatures generated from these groups are assigned based on three observations: (1) The spectrum collected from c-LA-PIMA-PEG shows only a peak at 7.9 ppm, which is ascribed to the amide group already present in the LA- $\text{NH}_2$  precursor (Figure 5D).<sup>24</sup> (2) However, the spectrum measured from o-LA-PIMA-PEG has two types of amide proton signatures, one at  $\sim 7.9\text{ ppm}$  ascribed to the pre-existing amide bond in LA groups and the other at 8.7 ppm corresponding to the newly formed bonds linking the LA/PEG blocks to the backbone during the ring opening transformation. The latter signature is conspicuously absent from the c-LA-PIMA-PEG spectrum (see profile Figure 5D), which confirms the cyclic imide formation for reactions carried out under high temperature conditions. Additionally, the  $^1\text{H}$  NMR spectrum collected from the c-PIMA-PEG (no LA) shows that the proton signals from  $-\text{CONH}-$  and  $-\text{COOH}$  are essentially negligible, confirming a closed ring structure (Figure 5E).

The above findings are supported by the information extracted from the HSQC data. The presence of two cross-peaks in Figure 5F confirms that the two amide protons at 8.7 and 7.9 ppm, measured for o-LA-PIMA-PEG (profile Figure 5C), are indeed associated with nitrogen in the  $^{15}\text{N}-^1\text{H}$  HSQC spectrum. Additionally, the nitrogen signal corresponding to the proton at 8.7 ppm is rather weak, a property that can be attributed to the slow exchange rate of proton on nitrogen with the carboxyl proton in its close proximity; such a result is common for amide groups.<sup>29</sup> The 2-D  $^{13}\text{C}-^1\text{H}$  HSQC spectrum collected from o-LA-PIMA-PEG shows that the above-mentioned protons, with  $\delta = 12.3, 8.7$ , and  $7.8\text{ ppm}$ , are not associated with any carbon atoms (Figure 5G), and must emanate from the O–H and N–H groups instead, as assigned above. Nonetheless, the broad proton signature centered at 13.8 ppm measured for o-LA-PIMA-PEG (profile Figure 5C) is not associated with nitrogen or carbon, as shown in the two HSQC spectra; we rather ascribe this broad resonance to protons involved in intramolecular hydrogen bonding.<sup>30,31</sup> We should note that the 2-D spectrum in Figure 5G shows signatures at (6.8, 125) ppm and at (6.6, 130) ppm, which can be ascribed to impurities containing conjugated structures. In particular, butylated hydroxytoluene (BHT) which has  $^1\text{H}$  and  $^{13}\text{C}$  signatures at the above shifts is commonly found in organic solvents as a stabilizer.<sup>32</sup> BHT impurities may be the source for these signatures measured for our compounds. Nonetheless, the signature at (6.65, 70) ppm cannot be identified.



**Gel Electrophoresis Experiments.** Gel electrophoresis measurements exploit the availability of net charges in the probed specimen (e.g., a protein or a colloidal nanoparticle) to promote a displacement/migration of the materials across the gel pores under applied voltage. In the present case, such a measurement is well suited for differentiating between the two polymer transformations discussed above. A ring opening transformation would yield a polymer that presents several carboxyl groups, thus a net negative charge that can produce a sizable mobility shift of the ligand either alone or ligated onto the QDs, toward the anode. Conversely, a complete transformation involving substitution or ring closing reaction would, in principle, provide a neutral compound that should not exhibit a mobility shift. This hypothesis was tested using three configurations. In the first, a Texas Red dye-labeled polymer (o-TXR-PIMA-PEG) was prepared by reacting PIMA with  $\text{H}_2\text{N}$ -PEG and  $\text{H}_2\text{N}$ -TXR (under mild conditions, in DMF at 40 °C). In the second, o-LA-PIMA-PEG prepared under mild heating conditions was photoligated onto luminescent CdSe-ZnS QDs. The resulting solutions/dispersions were loaded onto an agarose gel and run for 30 min (see [Supporting Information](#) for more details). Similar experiments were carried out using QDs photoligated with c-LA-PIMA-PEG ligands, prepared using addition reaction carried out at 153 °C. In both cases, the fluorescence from the QDs or dye was used to visualize the polymer-coated QDs or TXR-labeled PIMA-PEG. [Figure 6A](#) shows a gel image, acquired under UV

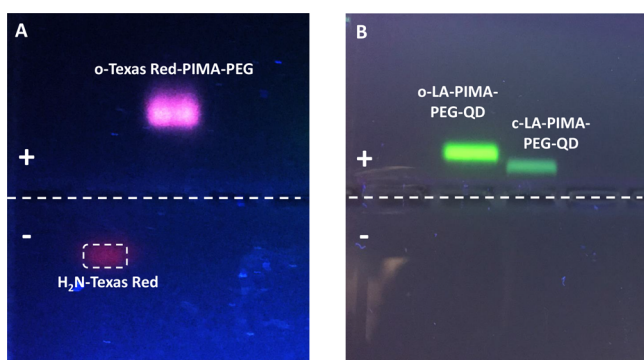


**Figure 6.** Agarose gel electrophoresis images collected (under fluorescence mode) from (A) free  $\text{H}_2\text{N}$ -Texas Red dye and o-TXR-PIMA-PEG prepared by reacting a  $\text{H}_2\text{N}$ -PEG- $\text{OCH}_3$  and  $\text{H}_2\text{N}$ -Texas Red with PIMA under mild conditions. (B) QDs photoligated with o-LA-PIMA-PEG (prepared under mild conditions), or with c-LA-PIMA-PEG (prepared in DMF under refluxing conditions). The dashed white lines designate the loading wells. The gels were run at 7.0 V/cm for 30 min (A) and at 6.5 V/cm for 30 min (B). The differences in the band PL intensities shown in both images are due to differences in the TXR or QD concentrations. The dashed rectangle is added to highlight the of amine-Texas-Red gel band.

excitation, simultaneously loaded with TXR-labeled PIMA-PEG and  $\text{H}_2\text{N}$ -TXR precursor (as control). The image shows that while the precursor exhibited a mobility toward the cathode, the o-TXR-PIMA-PEG polymer migrated toward the anode. This clearly proves that the addition reaction of PIMA with  $\text{H}_2\text{N}$ -PEG and  $\text{H}_2\text{N}$ -TXR mixture produces a net negative charge, ascribed to the carboxyl groups freed during the ring opening reaction, combined with consumption (via acylation) of all the amine groups in the  $\text{H}_2\text{N}$ -TXR precursor. The gel image in [Figure 6B](#) shows that QDs photoligated with o-LA-PIMA-PEG produced materials with a pronounced

mobility toward the anode, indicating that these QDs present several carboxyl groups; these were generated along the polymer chain during the addition reaction. This agrees well with the data shown for o-TXR-PIMA-PEG above. However, the image also shows that the dispersion of QDs photoligated with c-LA-PIMA-PEG also migrated toward the anode, albeit with a smaller mobility shift than that measured for the o-LA-PIMA-PEG-QDs. The smaller yet sizable mobility shift measured for c-LA-PIMA-PEG-QDs implies that the ligands on the QDs present several carboxylate groups, presumably a larger number than those measured in the c-LA-PIMA-PEG ligand prepared at high temperature (shown in the FT-IR data, [Figure 2](#)). The gel image in [Figure 6B](#) thus suggests that additional carboxyl groups may have been generated during the photoligation and phase transfer to buffer media, e.g., the running buffer, due to hydrolysis of the cyclic imides. Note that hydrolysis of cyclic imides in polymer materials under alkaline conditions has been reported by a few groups.<sup>33,34</sup>

Overall, combining the FT-IR, NMR, and gel electrophoresis data allows us to conclude that addition reaction carried out under mild conditions produces polymers featuring labile protons such as  $-\text{COOH}$  and  $-\text{CONH}-$ , while a cyclic imide transformation is favored under high temperatures or in the presence of  $\text{SOCl}_2$ . Nonetheless, our data also show that reaction carried out in methanol solution under refluxing conditions and for an extended period of time can increase the degree of imidization.

Finally, we would like to note that differences in the polymer transformations accompanying the addition (or substitution) reaction also manifest in the optical properties of the resulting compounds. For instance, we found that polymers presenting a closed ring structure (c-X) exhibit blue fluorescence emission. In contrast, compounds with open structure (o-X) have essentially negligible fluorescence.<sup>35,36</sup> The emission from c-X is visible under UV excitation using a hand-held UV lamp (see [Figure 7A](#) inset). [Figure 7A](#) also shows that the water solutions of c-PIMA-PEG and c-LA-PIMA-PEG exhibit broad photoluminescence profiles, with a maximum at  $\sim 438$ – $444$  nm, while emission from o-LA-PIMA-PEG is negligible. We should note that the PL profile collected from QDs photoligated with c-LA-PIMA-PEG solution exhibits a small shoulder at  $\sim 445$  nm, which emanates from the ligand contribution (see [Supporting Information, Figure S4](#)). This shoulder has not been measured for dispersions of QDs ligated with the o-LA-PIMA-PEG.<sup>6</sup> The absorption and excitation profiles collected from those polymers also show slight differences associated with their chemical structures ([Figure 7B](#)). In particular, the spectra collected from c-PIMA-PEG and c-LA-PIMA-PEG (red and blue curves) have a broad absorption peak at 294 nm, attributed to the presence of cyclic imides.<sup>37</sup> In comparison, the compounds o-LA-PIMA-PEG (green curve) does not exhibit the feature at 294 nm, indicating the absence of cyclic imide structures. In addition, the spectra collected from c-LA-PIMA-PEG and o-LA-PIMA-PEG (blue and green curves) exhibit a broad band at 324 nm ascribed to the dithiolane ring (in the oxidized lipoic acid).<sup>38,39</sup> Finally, additional excitation spectra were collected from PIMA, c-LA-PIMA-PEG, and o-LA-PIMA-PEG. The spectra show a broad excitation peak at 294 nm for the compounds containing imide rings in their structures ([Figure S5](#)).



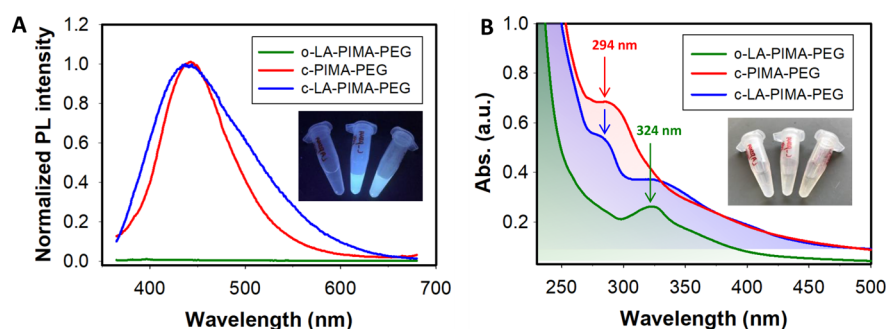


**Figure 7.** (A) Photoluminescence (PL) spectra of o-LA-PIMA-PEG (green), c-PIMA-PEG (red), and c-LA-PIMA-PEG (blue) in water solutions, excited at 350 nm; concentration  $\approx 2.5$  mg/mL; a fluorescent image of the samples under a hand-held UV lamp is shown in the inset. (B) Absorption spectra collected from the same three polymer solutions, with a white light image of the solutions shown in the inset.

## CONCLUSION

The addition reaction between poly(maleic anhydride)-based polymers and  $H_2N-R$  nucleophiles has gained interest recently; it has been used for preparing various multifunctional polymers. We have combined several characterization techniques to probe the nature of the transformation that occurs during the reaction between poly(isobutylene-*alt*-maleic anhydride) and  $H_2N-R$  ( $R$  = lipoic acid and/or PEG block) to prepare hydrophilic coordinating polymers. Our results show that under mild reaction conditions (in DMF at 65 °C) the reaction proceeds via ring opening transformation, yielding a o-LA-PIMA-PEG compound with amide-bound lateral groups. Conversely, a substitution reaction leading to the insertion of lateral  $R$  groups linked via cyclic imide rings occurs under higher temperature conditions (refluxing in DMF). We also found that refluxing in methanol or/and addition of  $SOCl_2$  can promote an imidization reaction (albeit partial) of pre-synthesized o-LA-PIMA-PEG ligand. The characteristic carbonyl signal from the anhydride rings, carboxylate groups, amide bonds, and cyclic imides are systematically identified using a combination of FT-IR and  $^1H$  NMR spectroscopy measurements. Gel electrophoresis experiments were further exploited to correlate the presence of carboxyl groups with mobility shifts of QDs photoligated with the modified PIMA polymers or TXR-labeled PIMA-PEG. Given the increased interest of nanomaterial surface functionalization, we believe that multifunctional coordinating polymer ligands prepared through the addition reaction between polymers containing the succinic anhydride motif (e.g., PIMA) and  $H_2N-R$  nucleophiles, carried out under either set of conditions, will find increasing use in developing biocompatible nanomaterials for applications in biotechnology and medicine.

## ASSOCIATED CONTENT

### Supporting Information

The Supporting Information is available free of charge on the ACS Publications website at DOI: 10.1021/acs.bioconjchem.9b00008.

Materials, instrumentation, compound synthesis, assignment of FT-IR features, ligand exchange,  $^1H$  NMR characterization, data and analysis (PDF)

## AUTHOR INFORMATION

### Corresponding Author

\*E-mail: mattoussi@chem.fsu.edu.

## ORCID

Wentao Wang: 0000-0003-2273-4171

Hedi Mattoussi: 0000-0002-6511-9323

## Present Addresses

<sup>†</sup>ASAHI-KASEI Corporation, Healthcare R&D Center, 2–1 Samejima, Fuji City, Shizuoka, 416–8501 Japan

<sup>‡</sup>DNA Electronics, Inc., 1891 Rutherford Road, Suite 100, Carlsbad, California 92008, USA

<sup>§</sup>The Food and Drug Administration, National Center for Toxicological Research, 3900 NCTR Road, Jefferson, Arkansas 72079, USA

## Notes

The authors declare no competing financial interest.

## ACKNOWLEDGMENTS

The authors thank FSU, the National Science Foundation (NSF-CHE #150850), the National Institutes of Health (NIH # R01 DC013080) and Asahi-Kasei, Inc. for financial support.

## REFERENCES

- (1) Lin, C. A.; Sperling, R. A.; Li, J. K.; Yang, T. Y.; Li, P. Y.; Zanella, M.; Chang, W. H.; and Parak, W. J. (2008) Design of an amphiphilic polymer for nanoparticle coating and functionalization. *Small* 4, 334–341.
- (2) Moghadam, P. N.; Azaryan, E.; and Zeynizade, B. (2010) Investigation of Poly(styrene-*alt*-maleic anhydride) Copolymer for Controlled Drug Delivery of Ceftriaxone Antibiotic. *J. Macromol. Sci., Part A: Pure Appl. Chem.* 47, 839–848.
- (3) Uppu, D. S. S. M.; Akkapeddi, P.; Manjunath, G. B.; Yarlagadda, V.; Hoque, J.; and Haldar, J. (2013) Polymers with tunable side-chain amphiphilicity as non-hemolytic antibacterial agents. *Chem. Commun.* 49, 9389–9391.
- (4) Peng, E.; Choo, E. S. G.; Sheng, Y.; and Xue, J. M. (2013) Monodisperse transfer of superparamagnetic nanoparticles from non-polar solvent to aqueous phase. *New J. Chem.* 37, 2051–2060.
- (5) Ravula, T.; Hardin, N. Z.; Ramadugu, S. K.; and Ramamoorthy, A. (2017) pH Tunable and Divalent Metal Ion Tolerant Polymer Lipid Nanodiscs. *Langmuir* 33, 10655–10662.
- (6) Wang, W.; Kapur, A.; Ji, X.; Safi, M.; Palui, G.; Palomo, V.; Dawson, P. E.; and Mattoussi, H. (2015) Photoligation of an Amphiphilic Polymer with Mixed Coordination Provides Compact and Reactive Quantum Dots. *J. Am. Chem. Soc.* 137, 5438–5451.
- (7) Janczewski, D.; Tomczak, N.; Han, M.-Y.; and Vancso, G. J. (2009) Stimulus Responsive PNIPAM/QD Hybrid Microspheres by Copolymerization with Surface Engineered QDs. *Macromolecules* 42, 1801–1804.
- (8) Wang, W.; Ji, X.; Kapur, A.; Zhang, C.; and Mattoussi, H. (2015) A Multifunctional Polymer Combining the Imidazole and Zwitterion

Motifs as a Biocompatible Compact Coating for Quantum Dots. *J. Am. Chem. Soc.* 137, 14158–14172.

(9) Wang, W., Ji, X., Burns, H., and Mattoussi, H. (2016) A multi-coordinating polymer ligand optimized for the functionalization of metallic nanocrystals and nanorods. *Faraday Discuss.* 191, 481–494.

(10) Wang, W., Ji, X., Du, L., and Mattoussi, H. (2017) Enhanced Colloidal Stability of Various Gold Nanostructures Using a Multi-coordinating Polymer Coating. *J. Phys. Chem. C* 121, 22901–22913.

(11) Karakuş, G. (2016) Synthesis, Structural Characterization, and Water Solubility of a Novel Modified Poly(maleic anhydride-co-vinyl acetate)/Acridine Conjugate. *Hacettepe J. Biol. & Chem.* 44, 549–558.

(12) Pellegrino, T., Manna, L., Kudera, S., Liedl, T., Koktysh, D., Rogach, A. L., Keller, S., Rädler, J., Natile, G., and Parak, W. J. (2004) Hydrophobic Nanocrystals Coated with an Amphiphilic Polymer Shell: A General Route to Water Soluble Nanocrystals. *Nano Lett.* 4, 703–707.

(13) Yu, W. W., Chang, E., Falkner, J. C., Zhang, J., Al-Somali, A. M., Sayes, C. M., Johns, J., Drezek, R., and Colvin, V. L. (2007) Forming Biocompatible and Nonaggregated Nanocrystals in Water Using Amphiphilic Polymers. *J. Am. Chem. Soc.* 129, 2871–2879.

(14) Wang, W., Ji, X., Na, H. B., Safi, M., Smith, A., Palui, G., Perez, J. M., and Mattoussi, H. (2014) Design of a Multi-Dopamine-Modified Polymer Ligand Optimally Suited for Interfacing Magnetic Nanoparticles with Biological Systems. *Langmuir* 30, 6197–6208.

(15) Li, M.-J., Bertocchi, M. J., and Weiss, R. G. (2017) Photophysics of Pyrenyl-Functionalized Poly(isobutylene-alt-maleic anhydride) and Poly(isobutylene-alt-maleic N-alkylimide). Influence of Solvent, Degree of Substitution, and Temperature. *Macromolecules* 50, 1919–1929.

(16) Schmidt, U., Stefan, Z., and Carsten, W. (2003) Modification of poly(octadecene alt maleic anhydride) films by reaction with functional amines. *J. Appl. Polym. Sci.* 87, 1255–1266.

(17) Vermeesch, I., and Groeninckx, G. (1994) Chemical modification of poly(styrene-co-maleic anhydride) with primary N-alkylamines by reactive extrusion. *J. Appl. Polym. Sci.* 53, 1365–1373.

(18) Song, S., Liu, L., and Zhang, J. (2011) Annealing improves tribological property of poly(octadecene-alt-maleic anhydride) self-assembled film. *Appl. Surf. Sci.* 257, 10254–10260.

(19) Liu, H.-Y., Yao, Z., Cao, K., and Li, B.-G. (2010) Kinetic analysis of the imidization of poly(styrene-co-maleic anhydride) with aniline in the melt. *J. Appl. Polym. Sci.* 116, 2951–2957.

(20) Socrates, G. (2001) *Infrared and Raman characteristic group frequencies: Tables and Charts*, 3rd ed., Wiley, Chichester, New York.

(21) Gu, X., and Yang, C. Q. (2000) FTIR Spectroscopy Study of the Formation of Cyclic Anhydride Intermediates of Polycarboxylic Acids Catalyzed by Sodium Hypophosphite. *Text. Res. J.* 70, 64–70.

(22) Colthup, N. B., Daly, L. H., and Wiberley, S. E. (1990) *Introduction to Infrared and Raman Spectroscopy*, 3rd ed., Academic Press, San Diego, CA.

(23) Mayer, C. K. K. (2012) Poly(alkyl-phosphonates), a modular approach to functionalization of surfaces, Ph.D. Thesis, ETH Zurich, Zurich, Switzerland.

(24) Susumu, K., Oh, E., Delehanty, J. B., Blanco-Canosa, J. B., Johnson, B. J., Jain, V., Hervey, W. J., Algar, W. R., Boeneman, K., Dawson, P. E., et al. (2011) Multifunctional Compact Zwitterionic Ligands for Preparing Robust Biocompatible Semiconductor Quantum Dots and Gold Nanoparticles. *J. Am. Chem. Soc.* 133, 9480–9496.

(25) Clayden, J., Greeves, N., Warren, S., and Wothers, P. (2001) *Organic Chemistry*, Oxford University Press, New York.

(26) Leggio, A., Belsito, E. L., De Luca, G., Di Gioia, M. L., Leotta, V., Romio, E., Siciliano, C., and Liguori, A. (2016) One-pot synthesis of amides from carboxylic acids activated using thionyl chloride. *RSC Adv.* 6, 34468–34475.

(27) Perry, S. J. (2000) *Investigation into the functionalisation of polyisobutylene*, Ph.D. Thesis, University of York.

(28) Zhao, E., Lam, J. W. Y., Meng, L., Hong, Y., Deng, H., Bai, G., Huang, X., Hao, J., and Tang, B. Z. (2015) Poly[(maleic anhydride)-

alt-(vinyl acetate)]: A Pure Oxygenic Nonconjugated Macromolecule with Strong Light Emission and Solvatochromic Effect. *Macromolecules* 48, 64–71.

(29) Silverstein, R. M., Webster, F. X., and Kiemle, D. J. (2005) *Spectrometric identification of organic compounds*, 7th ed., John Wiley & Sons, Hoboken, NJ.

(30) Abraham, M. H., and Abraham, R. J. (2017) A simple and facile NMR method for the determination of hydrogen bonding by amide N–H protons in protein models and other compounds. *New J. Chem.* 41, 6064–6066.

(31) Wöhnert, J., Dingley, A. J., Stoldt, M., Görlach, M., Grzesiek, S., and Brown, L. R. (1999) Direct identification of NH...N hydrogen bonds in non-canonical base pairs of RNA by NMR spectroscopy. *Nucleic Acids Res.* 27, 3104–3110.

(32) Gottlieb, H. E., Kotlyar, V., and Nudelman, A. (1997) NMR Chemical Shifts of Common Laboratory Solvents as Trace Impurities. *J. Org. Chem.* 62, 7512–7515.

(33) Khan, M. N., and Khan, A. A. (1975) Kinetics and mechanism of hydrolysis of succinimide in highly alkaline medium. *J. Org. Chem.* 40, 1793–1794.

(34) Stephans, L. E., Myles, A., and Thomas, R. R. (2000) Kinetics of Alkaline Hydrolysis of a Polyimide Surface. *Langmuir* 16, 4706–4710.

(35) Song, G., Lin, Y., Zhu, Z., Zheng, H., Qiao, J., He, C., and Wang, H. (2015) Strong Fluorescence of Poly(N-vinylpyrrolidone) and Its Oxidized Hydrolyzate. *Macromol. Rapid Commun.* 36, 278–285.

(36) Yan, J., Zheng, B., Pan, D., Yang, R., Xu, Y., Wang, L., and Yang, M. (2015) Unexpected fluorescence from polymers containing dithio/amino-succinimides. *Polym. Chem.* 6, 6133–6139.

(37) Gandini, A., Coelho, D., Gomes, M., Reis, B., and Silvestre, A. (2009) Materials from renewable resources based on furan monomers and furan chemistry: Work in progress. *J. Mater. Chem.* 19, 8656–8664.

(38) Barltrop, J. A., Hayes, P. M., and Calvin, M. (1954) The Chemistry of 1,2-Dithiolane (Trimethylene Disulfide) as a Model for the Primary Quantum Conversion Act in Photosynthesis I. *J. Am. Chem. Soc.* 76, 4348–4367.

(39) Mishra, D., Wang, S., Michel, S., Palui, G., Zhan, N., Perng, W., Jin, Z., and Mattoussi, H. (2018) Photochemical transformation of lipoic acid-based ligands: probing the effects of solvent, ligand structure, oxygen and pH. *Phys. Chem. Chem. Phys.* 20, 3895–3902.